Structural Reorganization of the Acetylcholine Binding Site of the *Torpedo* Nicotinic Receptor as Revealed by Dynamic Photoaffinity Labeling

Thomas Grutter,*[a, b] Sonia Bertrand,[c] Florence Kotzyba-Hibert,[b] Daniel Bertrand,[c] and Maurice Goeldner[b]

We explored the structural changes that occur at the acetylcholine binding site of the Torpedo marmorata *nicotinic receptor during activation by the tritiated photoactivatable agonist (diazocyclohexadienoylpropyl)trimethylammonium ([^{3}H]DCTA). We quantified the incorporation of radioactivity into the receptor subunits as a function of the mixing time of [^{3}H]DCTA with the receptor by using a rapid-mixing device adapted with a photochemical quenching system. A saturable increase of the specific photolabeling on the α and γ subunits was observed with a half-time of about 2 minutes. We further analyzed this photoincorporation either after rapid mixing for 500 ms or after equilibration for 50 minutes. Under these conditions, [^{3}H]DCTA explored transient state(s) and the stable desensitized state, respectively. Comparative analyses showed that at a probe concentration of 10 μM the relative variation of photoincorporation was more pronounced for the γ subunit (three- to fourfold) than for the α subunit (about twofold). By contrast, the relative distribution of radioactivity among α-subunit labeled residues (αTyr190, αCys192, αCysC193, and αTyr198) did not change. Altogether, these results reveal that during the course of agonist-induced receptor desensitization, the site-lining peptide loops, which belong to adjacent α and γ subunits, move closer to each other.*

KEYWORDS:

allosterism · photoaffinity labeling · receptors · structure – activity relationships

Introduction

The nicotinic acetylcholine receptor (nAChR) from fish electric organs and vertebrate neuromuscular junctions is a well-characterized transmembrane allosteric protein[1] composed of four polypeptide chains assembled into a heterologous $(\alpha1)_2(\beta1)\gamma\delta$ pentamer that carries the acetylcholine (ACh) binding sites and contains the cation-selective channel-forming elements.[2] The molecular structure of the *Torpedo marmorata* ACh binding site has been probed by site-directed irreversible photolabeling experiments by using photosensitive reagents (for a review, see Ref.[3]). These studies identified three domains of the α subunit centered around loop A (αTyr-93), loop B (αTrp-149), and loop C (αTyr-190, αCys-192, αCys-193, αTyr-198) that form the main part of the binding site whilst two complementary domains were identified on the γ and δ subunits in loop D (γTrp-55, δTrp-57) and loop E (γLeu-109, γTyr-111, γTyr117, δLeu-111). All these data were recently confirmed by the resolution at the atomic level of a homopentameric homologue of the N-terminal extracellular domain of the nicotinic receptor[4] (see Figure 1). The structure of this acetylcholine-binding protein (AChBP), synthesized in the glial cells in the brain of the snail *Lymnaea stagnalis*,[5] revealed the atomic arrangement of the amino acids that frame the acetylcholine binding site of nicotinic receptors.[4]

nAChR is a protein that undergoes allosteric transitions upon agonist binding.[1] At least four discrete interconvertible conformational states have been characterized. These states are called the resting (R), active (A; with the channel open), intermediate (I), and desensitized (D) states, respectively (Figure 2A). Agonist binding causes the channel to open (A) followed by rapid (I) and slow (D) desensitization of the receptor after prolonged exposure to the agonist.

Time-resolved photolabeling experiments were carried out on the *Torpedo* nicotinic receptor with photolabile noncompetitive

[a] *Dr. T. Grutter*
Correspondence address:
Laboratoire "Récepteurs et Cognition"
Institut Pasteur, 25 rue du Dr. Roux
75724 Paris Cedex 15 (France)
Fax: (+33) 1-4568-8836
E-mail: grutter@pasteur.fr

[b] *Dr. T. Grutter, Dr. F. Kotzyba-Hibert, Prof. Dr. M. Goeldner*
Laboratoire de Chimie Bioorganique
Université Louis Pasteur, Strasbourg (France)

[c] *Dr. S. Bertrand, Prof. Dr. D. Bertrand*
Laboratoire de Physiologie, CMU
Faculté de Médecine
1 rue Michel Servet, 1211 Geneva 4 (Switzerland)

  1439-4227/02/03/07 $ 20.00+.50/0 ChemBioChem **2002**, 3, 652 – 658

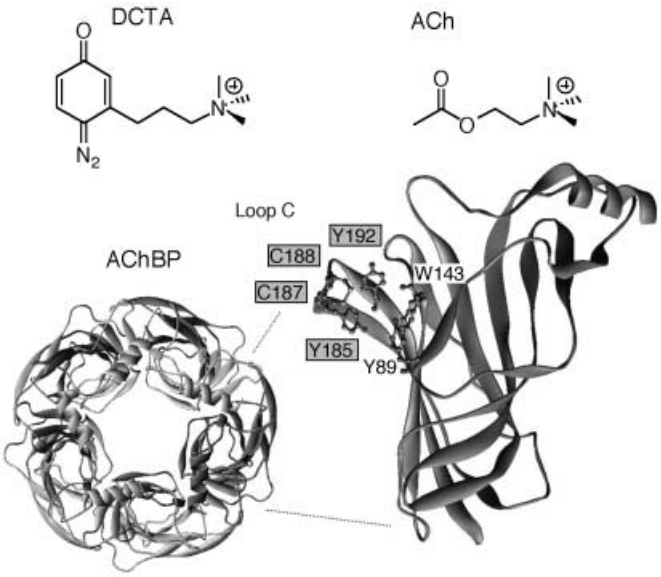

Figure 1. *Top: Chemical structures of the agonists (diazocyclohexadienoylpropyl)trimethylammonium (DCTA) and ACh. Bottom: Crystal structure of AChBP (PDB entry 1I9B); left, pentameric arrangement; right, structure of a monomer. The ball-and-stick representation corresponds to amino acids identified by photoaffinity labeling of the* Torpedo *α subunit. DCTA-labeled residues in the desensitized state of the* Torpedo *receptor are in shaded boxes.[16] The numbering refers to the AChBP sequence. The figure was constructed with Swiss-PbdViewer.[23]*

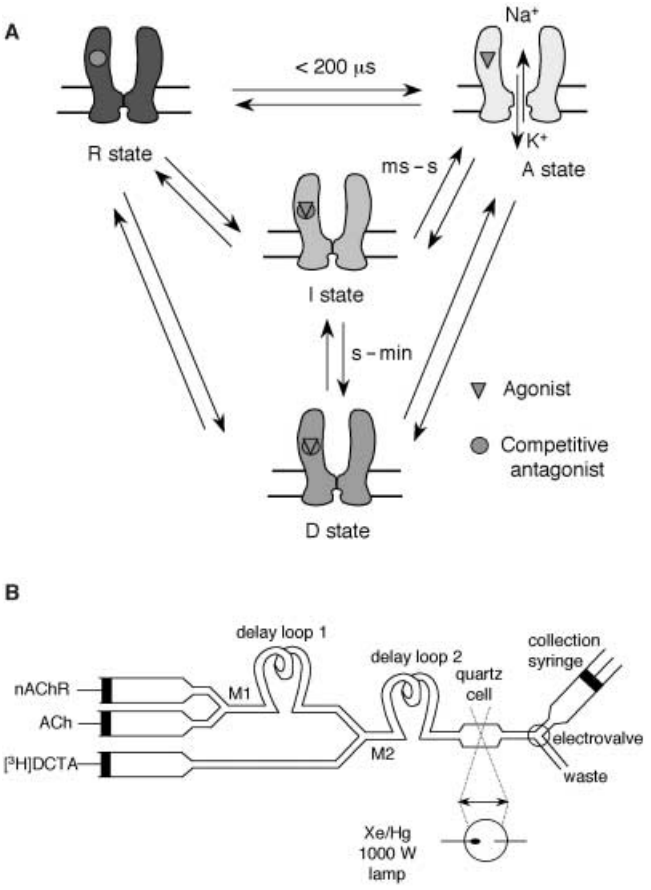

Figure 2. *A) Four-state model of nAChR. Upon binding of the agonist, the receptor isomerizes (less than 200 μs) from the low affinity resting (R) state to the intermediate-affinity active (A) state. Prolonged exposure to the agonist induces rapid (ms to s) and slow (s to min) desensitization of the receptor towards high- (I) and very-high-affinity (D) states. Agonist stabilizes the active and the desensitized states whereas competitive antagonist stabilizes the closed resting and desensitized states. B) Schematic drawing of the rapid-mixing device adapted for photoaffinity labeling. The different reactants were loaded into three syringes, rapidly mixed in chambers M1 and M2, and delayed in loops before being irradiated with UV light in the quartz cell. Samples were collected in the collection syringe.*

antagonists[6–12] and with the competitive photosensitive antagonist [^{3}H]*p*-(*N*,*N*-dimethylamino)-benzenediazonium fluoroborate ([^{3}H]DDF).[13] In the [^{3}H]DDF study, the authors reported that during the R→D transition of the receptor, photoincorporation into the α and δ subunits increased and a decrease of photolabeling on the γ subunit was observed. This conformational transition was characterized by an increase in the labeling of residues αTyr-93 (loop A) and αTrp-149 (loop B), which demonstrates a reorganization of the tertiary and/or quaternary structure at the level of the ACh binding site during the desensitization of the receptor. Unfortunately the antagonist character of the DDF molecule meant that this probe could not be used to explore functional states of the nicotinic receptor. Accordingly, we developed a novel family of photosensitive agonists of suitable size and reactivity, designed to be covalently incorporated amongst the surrounding ACh-binding residues upon UV irradiation.[14] One of these photoprobes, DCTA (Figure 1) is a functional agonist of nAChR that is expressed by TE 671 cells[15] and was designed to explore the ester-binding pocket of ACh.[16] The four [^{3}H]DCTA-labeled residues (Tyr-190, Cys-192, Cys-193, and Tyr-198) in the receptor were anticipated to participate directly in the binding of the ester moiety of ACh. In view of the crystal structure of AChBP, the corresponding residues (Tyr-185, Cys-187, Cys-188, and Tyr-192) are in close proximity to these [^{3}H]DCTA-labeled species (Figure 1).

In this work, we investigated dynamic photolabeling of the *Torpedo marmorata* nicotinic receptor with [^{3}H]DCTA. We explored for the first time the structural changes that occur at the ACh binding site during cholinergic activation by quantification of the photoincorporated radioactivity into the receptor subunits and subsequently into the labeled amino acids as a function of mixing times. In particular, we selected mixing times of 500 ms and 50 min, which enabled the ACh binding site to be photolabeled in the intermediate I and desensitized D states, respectively. The labeling analyses suggest that during the slow I→D transition of the receptor, the loops that form the ACh binding site on the α and γ subunits move closer to each other. This structural reorganization, revealed by time-resolved photolabeling experiments with [^{3}H]DCTA, provides access to a possible model of the allosteric transitions that occur on the ACh binding site.

Results

Kinetic analysis of the photoincorporation of [^{3}H]DCTA

In a previous study we solved the problem of nonspecific labeling in [^{3}H]DCTA photolabeling experiments on nAChR-rich

membranes by subsequent addition of the oxidant ceric ion (Ce^{IV}) and glutathione (GSH) to quench the undesired reactions.[17] We applied these conditions to the rapid mixing experiments by addition of a quenching solution (500 μM Ce^{IV}/250 μM GSH, final concentrations, Figure 2B) to the collection syringe.

In the first series of experiments we analyzed the photoincorporation of the agonist [^{3}H]DCTA into the acetylcholine binding site of the *Torpedo* receptor as a function of mixing times, which ranged from 500 ms to 1 hour (Figure 3A). A twofold increase in the radioactivity in both α and γ subunits was quantified by SDS-PAGE (see the Experimental Section). Since the same amount of protein was loaded onto the gels in each case, this increase in radioactivity reflects an increase in labeling. Specific photolabeling (determined in the presence of an excess of carbamylcholine (CCh)) mainly occurred on the α subunit (90%) while minor labeling of the γ subunit (10%) was consistently observed, independent of the mixing time (Figure 3B). In the absence of light, no significant incorporation of the radioactive label was measured on either α or γ chains (data not shown), which demonstrates that the specific increase of radioactivity incorporation is UV light dependent. Together these data indicate that the dynamic photoincorporation of [^{3}H]DCTA occurs specifically within the ACh binding domain. A thirtyfold excess of [^{3}H]DCTA over [^{125}I]α-bungarotoxin binding sites was used to favor a pseudo-first-order reaction mechanism and under these conditions the time-dependent radioactivity incorporation at the α and γ subunits fits a single exponential rate equation. A slight difference in the half-life of the photoincorporation was observed between the α ($t_{1/2} \sim 2$ min) and γ subunits ($t_{1/2} \sim 0.5$ min).

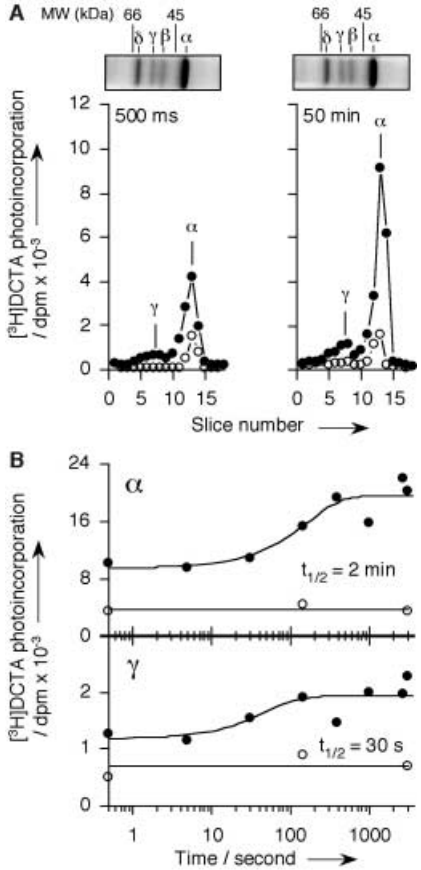

Figure 3. *Photoincorporation of [^{3}H]DCTA as a function of mixing time. A) SDS-PAGE analysis of [^{3}H]DCTA (10 μM) photoincorporation into alkaline-treated nAChR after 500 ms (left) rapid mixing without preincubation with ACh, or (right) at equilibrium (50 min) in the absence (●) or presence (○) of 200 μM CCh. The samples were UV irradiated (< 30 ms) and collected in the collection syringe, which was prefilled with the quenching solution (Ce^{IV}/GSH). The alkylated membranes were centrifuged and pellets were subjected to 10% SDS-PAGE. Distribution of the radioactivity into each subunit was measured after gel slicing, digestion, and counting. Coomassie-stained gels that indicate the radioactivity distribution are shown. Also indicated are the positions of the four nAChR subunits and the molecular weight markers (MW in kDa). B) Kinetics of [^{3}H]DCTA (10 μM, 10 °C) photoincorporation into the α and γ subunits in the absence (●) or presence (○) of 200 μM CCh. The solid lines are the best fit of a single exponential rate equation through the data points (●). dpm = disintegrations per minute.*

Photolabeling of agonist-induced conformational states

Membranes were initially treated with ACh (0.6 μM final concentration in the first delay loop, see Figure 2B) for 450 ms to label agonist-induced conformational states of the receptor (R, A, and I). In the absence of effector this preincubation with ACh for 450 ms allows selective presaturation of the high-affinity sites in the D state (about 20% of the sites).[18, 19], which is necessary because there is a preexisting equilibrium between the resting and the desensitized states of the *Torpedo* receptor. Under these conditions, the agonist [^{3}H]DCTA labels states that can be activated other than the D state. Quantification of the labeling reaction in the presence of ACh showed that 97% of the photoincorporation occurred in the α subunit and 3% in the γ subunit at 10 μM probe concentration. In addition, over the concentrations of [^{3}H]DCTA tested, photolabeling reached saturation only for the α subunit (the apparent dissociation constant, $K_{app} = 25 \pm 9$ μM, Figure 4, open circles).

To predominantly label the desensitized state, we selected longer incubation times for the agonist [^{3}H]DCTA and the receptor. We tested different concentrations of [^{3}H]DCTA and as expected specific photolabeling reached saturation as the concentration of the probe was increased (Figure 4). The K_{app} values for specific photolabeling of the α- and γ subunits were 4.7 ± 0.2 and 5.6 ± 0.3 μM, respectively. The extent of nonspecific labeling (for example, in the presence of 200 μM CCh) was a linear function of [^{3}H]DCTA concentration up to at least 35 μM (data not shown).

Quantification of photolabeling of the different agonist-induced conformational states

To analyze at higher resolution the structural changes that occur in the α subunit after incubation with the agonist [^{3}H]DCTA, we compared the patterns of labeling in the different agonist-induced conformational states. First, we analyzed photoincorporation of the radiolabel into the proteolytic labeled peptides. As previously shown,[16] when the protein was labeled at equilibrium (50 min) a unique radioactive peak was observed by HPLC that results from specifically labeled overlapping α subunit proteolytic peptides. Half the amount of radioactivity

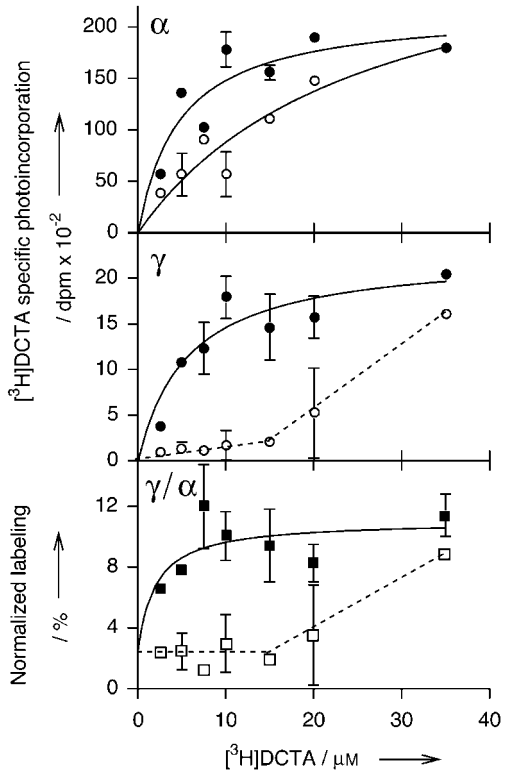

Figure 4. *Concentration dependence of [³H]DCTA photoincorporation into different states quantified for the α and γ subunits. ●, Specific [³H]DCTA photoincorporation (UV irradiation < 30 ms) after 50 min equilibration with alkaline-treated nAChR; ○, specific [³H]DCTA photoincorporation after 500 ms rapid mixing with alkaline-treated membranes presaturated with ACh for 450 ms (see the text for details). The specific photolabeling is given by the difference between the total photolabeling (in the absence of CCh) and the nonspecific labeling calculated from linear least-squares analysis of the experimental data (in the presence of CCh). The solid lines are the best fit for hyperbolic saturation curves. Labeling normalized according to that of the α subunit (γ/α) is also represented both at equilibrium (■) and after rapid-mixing (□).*

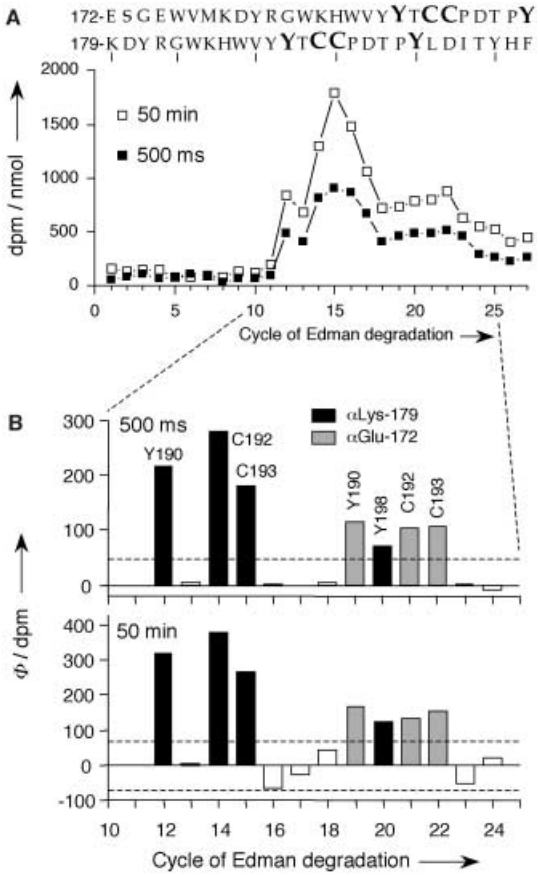

Figure 5. *A) Radioactivity released upon sequential Edman degradation of [³H]DCTA-labeled CNBr fragments. HPLC-purified material was subjected to automated sequence analysis. Radioactivity associated with the phenyl thiohydantoin (PTH) fraction at each cycle that corresponds to photolabeled receptor in the D state (□) or the I state (■) was normalized according to the total initial amount of loaded peptide (I_0 = 373 pmol for the D state and I_0 = 449 pmol for the I state). The two identified peptides, which extend from αLys-179 and αGlu-172 are shown (see also Table 1), and the radiolabeled amino acids are indicated in boldface type. B) Quantitative analysis of sequencing data from different mixing time conditions. Radioactivity release data were analyzed according to a mathematical model (see the Experimental Section) that integrates the observed lag at each cycle. When the Φ value is more than 25% (broken lines) of that of the first labeled residue (Y190), it is assumed that the residue in question is labeled at the corresponding cycle. Labeled residues that belong to the αLys-179 and αGlu-172 peptides are shown in black and grey bars, respectively. White bars correspond to unlabeled residues.*

was seen in the same peak position when irradiation was performed 500 ms after rapid mixing with nAChR-rich membranes presaturated with 0.6 μM ACh (data not shown).

Secondly, we analyzed photoincorporation at the amino acid level by using identical experimental procedures (cyanogen bromide (CNBr) cleavage in gel) for both conditions (that is, at equilibrium or at 500 ms) to avoid any possible misleading determination of the labeled residues. Sequence analysis of the radioactive peptides showed that the labeled loop C amino acids (αTyr-190, αCys-192, αCys-193, and αTyr-198) had incorporated radioactivity in the same proportions under both conditions, with a 1.7-fold overall radioactivity increase from 500 ms to 50 min (Figure 5 A and Table 1).

Sequencing data were analyzed according to a mathematical model that integrates the observed lag for each residue in the different cycles into the results (see the Experimental Section). Application of the model to the experimental data led to the following conclusions: 1) the labeling of all four residues, αTyr-190, αCys-192, αCys-193, and αTyr-198, by [³H]DCTA is confirmed; 2) αTyr-198 incorporates about half the amount of radioactivity compared to the three other amino acids labeled by [³H]DCTA; 3) the relative distribution of radioactivity among the four labeled residues does not change whatever mixing time conditions are used (Figure 5 B).

Attempts to identify labeled residues on the γ subunit at equilibrium failed because of low radioactivity incorporation.

Discussion

In the present study, we irreversibly labeled agonist-induced conformational states of the *Torpedo* nicotinic receptor with the tritiated photosensitive agonist [³H]DCTA, which targets the acetylcholine binding site. We explored different mixing times for the receptor and [³H]DCTA before flash photolysis of the incubation mixture was carried out. Initially, we tested shorter

Table 1. *Yields of PTH amino acids upon sequence analysis of CNBr peptides from the α subunit of nAChR labeled with [³H]DCTA.[a]*

	PTH amino acids [pmol]			
	500 ms after mixing (I state)		After 50 min equilibration (D state)	
cycle	I	II	I	II
1	K (NQ)	E (NQ)	K (NQ)	E (NQ)
2	D (37.7)	S (ND)	D (39.8)	S (ND)
3	Y (110.7)	G (48.0)[b]	Y (174.0)	G (60.7)[b]
4	R (29.7)	E (15.0)	R (34.2)	E (14.1)
5	G (78.7)	W (ND)	G (87.5)	W (ND)
6	W (ND)	V (16.2)	W (ND)	V (12.0)
7	K (41.1)	M (15.7)	K (34.8)	M (18.2)
8	H (32.0)	K (49.8)[b]	H (35.8)	K (46.9)[b]
9	W (ND)	D (5.8)	W (ND)	D (4.2)
10	V (27.5)	Y (140.2)[b]	V (56.2)	Y (148.2)[b]
11	Y (NQ)	R (5.1)	Y (NQ)	R (7.7)
12	Y (NQ)	G (11.3)	Y (NQ)	G (12.4)
13	T (11.1)	W (ND)	T (13.1)	W (ND)
14	C (ND)	K (2.9)	C (ND)	K (3.1)
15	C (ND)	H (3.9)	C (ND)	H (4.7)
16	P (16.9)[b]	W (ND)	P (10.5)[b]	W (ND)
17	D (4.7)	V (ND)	D (4.7)	V (ND)
18	T (ND)	Y (ND)	T (ND)	Y (ND)
19	P (32.0)[b]	Y (3.3)	P (24.0)[b]	Y (4.3)
20	Y (5.4)	T (ND)	Y (4.9)	T (ND)
21	L (0.4)	C (ND)	L (0.8)	C (ND)
22	D (7.8)[b]	C (ND)	D (7.9)[b]	C (ND)
23	I (5.9)	P (ND)	I (1.9)	P (ND)
24	T (ND)	D (ND)	T (0.2)	D (ND)
25	Y (2.4)	T (ND)	Y (7.7)	T (2.9)[b]
26	H (ND)	P (ND)	H (ND)	P (ND)
27	F (ND)	Y (ND)	F (ND)	Y (ND)
I_0 [pmol]	106.0	27.4	152.4	21.2
R [%]	84	88	82	91
starting position	αTyr-190	αCys-192	αTyr-190	αCys-192

[a] NQ indicates that the residue was detected but radioactivity was not quantified because detection was in the first cycle or because of carry over from the same residue present in a preceding cycle. ND indicates that the residue was not identified but deduced from the sequence. [a] Residues that were present in different sequences were not included in the linear regression analysis for the calculation of the repetitive yield R and initial amount I_0.

mixing times (8.5 – 100 ms). At 10 μM probe concentration we observed a very rapid photolabeling that took place on the ms timescale (not shown). Although an increase in radioactivity incorporation into the α and γ subunits could be reliably detected (up to tens of ms), the experimental errors were unfortunately too significant to allow confident conclusions. Therefore we limited this study to mixing times in the range 500 ms to one hour. We analyzed in more detail this second photoincorporation kinetic, which presented half-lives on the minute timescale. During this transition, an increase in radioactivity photoincorporation was observed in both the α and γ subunits (Figure 3). We studied the photoincorporation of the radioactive label into these subunits as a function of [³H]DCTA concentration under well-defined experimental conditions (Figure 4). We selected a very long agonist incubation time (50 min) to selectively label the desensitized state (D) of the receptor, whereas to label predominantly the agonist-induced conformational states (R, A, and I) we selected shorter incubation times (500 ms). It appeared that during the conformational transition of the receptor, the DCTA concentration markedly influenced incorporation into the γ subunit compared to the α subunit (Figure 4). The contribution of the γ subunit increased only at higher [³H]DCTA concentrations when the labeling was explored at 500 ms in the presence of a low concentration of ACh. Although the mechanism responsible for this last phenomenon remains to be elucidated, the result might be explained by an increased occupancy of the R state under these conditions (see Figure 2 A). Higher concentrations of the probe label the lower affinity R state, which results in increased labeling of the γ subunit, as was observed previously for labeling of the R state with the antagonist [³H]DDF.[13] While the active state (A) could not be analyzed within our experimental conditions, the radioactivity increase observed as a function of incubation time (Figure 3) is likely to correspond to the conformational transition between the intermediate (I) and the desensitized (D) state of the receptor (Figure 2 A).

Microsequencing analysis of the photoincorporation revealed that the residues αTyr-190, αCys-192, αCys-193, and αTyr-198 are the primary sites of photoincorporation of the agonist [³H]DCTA into the α subunit in both the intermediate and desensitized states (Figure 5). The amount of photoincorporation doubled for the four labeled residues with the conversion from the I to the D state (Figure 5 B). Quantitatively, as discussed earlier, residues αTyr-190, αCys-192, and αCys-193 are labeled with the same efficiency while the photoincorporation at residue αTyr-198 is approximately half as efficient (Figure 5 B). The possibility that some of the covalent bonds of the photoadduct could be labile under the microsequencing conditions cannot be ruled out, however the pattern of the radioactivity profile could reflect changes in proximity and/or accessibility of the probe to the labeled residues.

The identical relative increase of radioactivity incorporation into each of the α-subunit amino acid residues that was labeled during the I→D transition can readily be explained by an increase of ACh binding site occupancy by [³H]DCTA at the probe concentration used. However, this phenomenon cannot explain on its own the different radioactivity incorporation observed for the α and γ subunits (Figure 4). This difference suggests that, in addition to the affinity increase, a reorganization of the tertiary and/or quaternary structure of the protein occurs during the I→D transition. On the basis of the experimental data and with the assumption that the ligand binding sites are located at subunit interfaces, we propose that during the allosteric transition from the intermediate closed state to the desensitized closed state of the receptor, the α and γ subunits move together to tighten-up the ACh binding site (Figure 6).

The recent determination at 2.7 Å resolution of the crystal structure of the snail *Lymnaea stagnalis* acetylcholine binding protein, a structural and functional homologue of the N-terminal ligand binding domain of the nAChR α subunit, shows that the putative ACh binding sites are located at subunit boundaries.[4] It was postulated that the "compact" form of AChBP corresponds to the D state of the receptor.[20] The functional states would then result from the opening of the binding sites in a concerted clockwise rotation of all the subunits. Accordingly, transitions towards the D state would be accompanied by increased

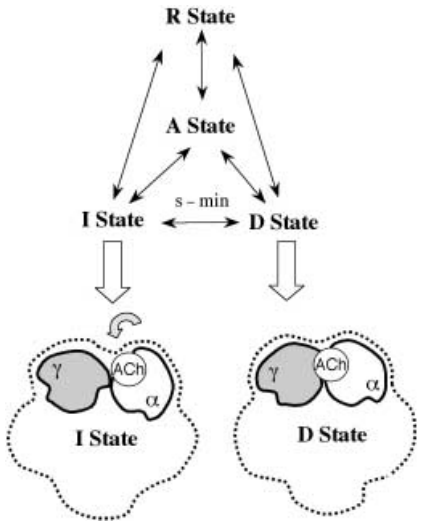

Figure 6. *Quaternary model of allosteric transitions in the [³H]DCTA-binding domain upon isomerization between the intermediate (I) and desensitized (D) states. See the text for a discusssion.*

interactions with the bound cholinergic agonist, which would lead to the affinity increase usually observed. In partial agreement with the present model, Galzi et al.[13] reported that during the R→D transition the receptor exhibited an increase in photoincorporation into the α and δ subunits, concomitant with decreased photolabeling of the γ subunit. Although these results appear to be in conflict with our results, we must take into account the following observations: 1) The two ACh binding sites in the *Torpedo* receptor are not structurally identical. Some of the peptide loops that frame the site in the γ and δ subunits, in particular in proximity to loop F, share low sequence identity, which creates different ACh binding cavities; 2) DCTA and DDF probed different conformational transitions, the I→D and R→D respectively; 3) the molecules used explore different ACh binding areas. Altogether these labeling studies describe different phenomena and should therefore not be analyzed comparatively. In conclusion this work emphasizes that dynamic photoaffinity labeling experiments represent a powerful tool to investigate structural changes that occur within a functional protein, especially when a high resolution 3D structure of the protein is available.

Experimental Section

Materials: [³H]DCTA (0.4 – 0.6 Ci mmol^{-1}) was synthesized and purified as described previously.[15] nAChR-rich membranes were purified from *T. marmorata* frozen electric organs as described elsewhere.[21] Further purification was achieved by alkali treatment of nAChR-rich membrane fragments.[22] CCh and GSH were purchased from Sigma. Cerium nitrate ammonium ($Ce^{IV}(NH_4)_2(NO_3)_6$) was purchased from Janssen.

Rapid-mixing photolabeling apparatus: The rapid-mixing photolabeling apparatus was constructed (Biologic, France) by combination of SFM-3 stopped-flow and optical quench apparatus with a 1000-Watt high-pressure Xe/Hg lamp (Osram) to deliver intense UV light as described previously.[6] The incident light beam was focused on a quartz cell (FC-15, 31 μL) to obtain maximum illumination. The rapid sequential mixing of up to three solutions was achieved in mixing chambers M1 and M2 (see Figure 2B) and was time-controlled by the MPS (mixer power-supply) module by using both continuous and interrupted modes and by variation of the length of the delay lines. The mixed solutions were irradiated with UV light as they passed through the quartz cell and collected in the collection syringe, which was prefilled with Ce^{IV}/GSH solution (250 μL). A 1 mL s^{-1} flow rate was selected, which corresponds to a duration of irradiation less than 30 ms.

Rapid-mixing photolabeling in the presence of ACh: All photolabeling experiments were performed at 10 °C in phosphate buffer (10 mM, pH 7.2). This low ionic strength was compatible with the use of Ce^{IV}/GSH treatment. Alkaline-treated nAChR-rich membranes (0.65 μM final concentration in delay loop 1) were first incubated with ACh (0.6 μM) for 450 ms to saturate the approximately 20% high-affinity D state that exists in the absence of any effector.[13] This solution (0.325 μM final concentration in delay loop 2) was mixed with [³H]DCTA for a chosen mixing time and irradiated. The sample was collected in the collection syringe and the photolysis products were quenched with Ce^{IV}/GSH in order to increase the specific photolabeling.[17]

Equilibrium photolabeling in the absence of ACh: Alkaline-treated nAChR-rich membranes were incubated in the dark in the presence of [³H]DCTA for 50 min at 10 °C then irradiated as described above by using the rapid-mixing apparatus. The irradiation conditions were thus identical to those of the rapid-mixing experiments.

Determination of the extent of photolabeling: Following photolabeling, membranes recovered from the collection syringe were centrifuged and samples were analyzed by 10% SDS-PAGE.[16] The amount of radioactive label incorporated into each polypeptide chain was quantified after gel slicing, digestion, and counting.[17]

CNBr cleavage and sequencing: After preparative irradiation of a large amount of alkaline-treated nAChR-rich membranes mixed with [³H]DCTA under different conditions, the α chains were isolated and cleaved by CNBr and the labeled peptides were purified by HPLC and sequenced as described.[16] For sequence analysis, initial peptide mass (I_0) and repetitive yields R were calculated by linear least-squares analysis of the function $\log I_n = n[\log R] + \log I_0$, where I_n is the observed mass of PTH amino acids released in cycle n.

Sequencing data analysis: We quantified the photoincorporation of radioactive label at the amino acid level according to a mathematical model developed in our laboratory. The model takes into account the lag which is observed in each cycle. We introduced the parameter Φ, which corresponds to the difference between the experimental lag (the observed release of radioactivity in each cycle; L_{exp}) and the calculated lag (L_{calc}, from the model), as described in Equations 1 and 2.

$$\Phi = L_{exp} - L_{calc} \quad (1)$$

$$L_{calc} = \sum_{p=1}^{n} A_{n,p} \quad (2)$$

In Equation 2, $A_{n,p}$ is the theoretical amount of each residue p released at the end of each cycle n and can be defined by Equation 3,

$$A_{n,p} = A_0 \frac{(n-1)!}{(p-1)! \times (n-p)!} \times R_p^p (1-R_p)^{(n-p)} \quad (3)$$

where A_0 represents the initial amount of peptide loaded and R_p is the repetitive yield associated with the cleavage of each residue. The

difference Φ represents the theoretical labeling if no lag were observed. We assumed that when Φ is greater than 25% of the extent of labeling of the first residue (here, Tyr-190, see Figure 5B), the residue is labeled at the corresponding cycle.

We thank Dr. L. Ehret-Sabatier and M. Leret for their skilful assistance during sequencing. We also thank Dr. P. J. Corringer and Dr. S. J. Edelstein for critically reading the manuscript.

[1] J. P. Changeux, S. J. Edelstein, *Neuron* **1998**, *21*, 959 – 980.
[2] F. Hucho, C. Weise, *Angew. Chem.* **2001**, *113*, 3194 – 3211; *Angew. Chem. Int. Ed.* **2001**, *40*, 3100 – 3116.
[3] F. Kotzyba-Hibert, T. Grutter, M. Goeldner, *Mol. Neurobiol.* **1999**, *20*, 45 – 59.
[4] K. Brejc, W. J. van Dijk, R. Klaassen, M. Schuurmans, J. van der Oost, A. B. Smit, T. K. Sixma, *Nature* **2001**, *411*, 269 – 276.
[5] A. B. Smit, N. I. Syed, D. Schaap, J. van der Minnen, J. Klumperman, K. S. Kits, H. Lodder, R. C. van der Schors, R. van Elk, B. Sorgedrager, K. Brejc, T. K. Sixma, W. P. M. Geraerts, *Nature* **2001**, *411*, 261 – 268.
[6] T. Heidmann, J. P. Changeux, *Proc. Natl. Acad. Sci. USA* **1984**, *81*, 1897 – 1901.
[7] T. Heidmann, J. P. Changeux, *Biochemistry* **1986**, *25*, 6109 – 6113.
[8] R. N. Cox, R. R. Kaldany, M. DiPaola, A. Karlin, *J. Biol. Chem.* **1985**, *260*, 7186 – 7193.
[9] M. DiPaola, P. N. Kao, A. Karlin, *J. Biol. Chem.* **1990**, *265*, 11 017 – 11 029.
[10] P. Muhn, A. Fahr, F. Hucho, *Biochemistry* **1984**, *23*, 2725 – 2730.
[11] G. H. Addona, M. A. Kloczewiak, K. W. Miller, *Anal. Biochem.* **1999**, *267*, 135 – 140.
[12] A. Fahr, L. Lauffer, D. Schmidt, M. P. Heyn, F. Hucho, *Eur. J. Biochem.* **1985**, *147*, 483 – 487.
[13] J. L. Galzi, F. Revah, F. Bouet, A. Menez, M. Goeldner, C. Hirth, J. P. Changeux, *Proc. Natl. Acad. Sci. USA* **1991**, *88*, 5051 – 5055.
[14] F. Kotzyba-Hibert, P. Kessler, V. Zerbib, C. Bogen, V. Snetkov, K. Takeda, M. Goeldner, C. Hirth, *J. Neurochem.* **1996**, *67*, 2557 – 2565.
[15] F. Kotzyba-Hibert, P. Kessler, V. Zerbib, T. Grutter, C. Bogen, K. Takeda, A. Hammadi, L. Knerr, M. Goeldner, *Bioconjugate Chem.* **1997**, *8*, 472 – 480.
[16] T. Grutter, L. Ehret-Sabatier, F. Kotzyba-Hibert, M. Goeldner, *Biochemistry* **2000**, *39*, 3034 – 3043.
[17] T. Grutter, M. Goeldner, F. Kotzyba-Hibert, *Biochemistry* **1999**, *38*, 7476 – 7484.
[18] N. D. Boyd, J. B. Cohen, *Biochemistry* **1980**, *19*, 5344 – 5353.
[19] T. Heidmann, J. P. Changeux, *Eur. J. Biochem.* **1979**, *94*, 255 – 279.
[20] T. Grutter, J. P. Changeux, *Trends Biochem. Sci.* **2001**, *26*, 459 – 463.
[21] T. Saitoh, J. P. Changeux, *Eur. J. Biochem.* **1980**, *105*, 51 – 62.
[22] R. R. Neubig, J. B. Cohen, *Biochemistry* **1980**, *19*, 2770 – 2779.
[23] N. Guex, M. C. Peitsch, *Electrophoresis* **1997**, *18*, 2714 – 2723.

Received: March 4, 2002 [F 377]